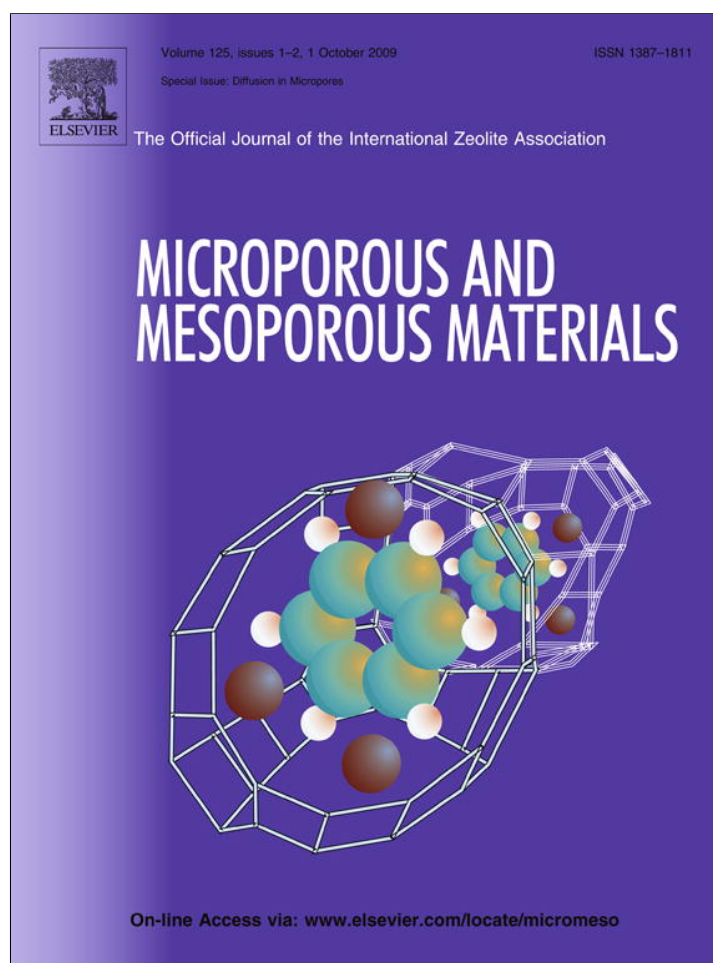


Provided for non-commercial research and education use.  
Not for reproduction, distribution or commercial use.



This article appeared in a journal published by Elsevier. The attached copy is furnished to the author for internal non-commercial research and education use, including for instruction at the authors institution and sharing with colleagues.

Other uses, including reproduction and distribution, or selling or licensing copies, or posting to personal, institutional or third party websites are prohibited.

In most cases authors are permitted to post their version of the article (e.g. in Word or Tex form) to their personal website or institutional repository. Authors requiring further information regarding Elsevier's archiving and manuscript policies are encouraged to visit:

<http://www.elsevier.com/copyright>



Contents lists available at ScienceDirect

## Microporous and Mesoporous Materials

journal homepage: [www.elsevier.com/locate/micromeso](http://www.elsevier.com/locate/micromeso)

## Diffusional and orientational dynamics of various single terylene diimide conjugates in mesoporous materials

Florian Feil<sup>a</sup>, Christophe Jung<sup>a</sup>, Johanna Kirstein<sup>a</sup>, Jens Michaelis<sup>a</sup>, Chen Li<sup>b</sup>, Fabian Nolde<sup>b</sup>, Klaus Müllen<sup>b</sup>, Christoph Bräuchle<sup>a,\*</sup><sup>a</sup>Department of Chemistry und Biochemistry and Center for Nanoscience (CeNS), Ludwig-Maximilians-Universität München, Butenandtstrasse 11, 81377 München, Germany<sup>b</sup>Max Planck Institute for Polymer Research, Ackermannweg 10, 55128 Mainz, Germany

## ARTICLE INFO

## Article history:

Received 10 November 2008

Received in revised form 22 January 2009

Accepted 23 January 2009

Available online 1 February 2009

With this publication we would like to honour Professor Dr. Jörg Kärger for his excellent contributions to the field of molecular diffusion over many years.

## Keywords:

Diffusion

Mesoporous materials

## ABSTRACT

Mesoporous silica materials are ideally suited as host–guest systems in nanoscience with applications ranging from molecular sieves, catalysts, nanosensors to drug-delivery-systems. For all these applications a thorough understanding of the interactions between the mesoporous host system and the guest molecules is vital. Here, we investigate these interactions using single molecule spectroscopy (SMS) to study the dynamics of three different terylene diimide (TDI) dyes acting as molecular probes in hexagonal and lamellar mesoporous silica films. The diffusion behaviour in the hexagonal phase is represented by the trajectories of the single molecules. These trajectories are highly structured and thus provide information about the underlying host structure, such as domain size or the presence of defects inside the host structure. The three structurally different TDI derivatives allowed studying the influence of the molecular structure of the guest on the translational diffusion behaviour in the hexagonal phase and the lamellar phase. In the lamellar phase, the differences between the three guests are quite dramatic. First, two populations of diffusing molecules – one with parallel orientation of the molecules to the lamellae and the other with perpendicular orientation – could be observed for two of the TDI derivatives. These populations differ drastically in their translational diffusion behaviour. Depending on the TDI derivative, the ratio between the two populations is different. Additionally, switching between the two populations was observed. These data provide new insights into host–guest interactions like the influence of the molecular structure of the guest molecules on their diffusional as well as on their orientational behaviour in structurally confined guest systems.

© 2009 Elsevier Inc. All rights reserved.

## 1. Introduction

Ordered mesoporous silica materials have recently advanced to an important field of research attracting interest not only in the scientific community, but also by the chemical industry as it offers many promising approaches for new high-tech materials. Indeed, they provide very interesting host systems for many inorganic, organic as well as biological guest molecules. Moreover, the wide range of possible sizes, topologies and polarity of these host systems allows for a specific design of the desired host–guest interactions. Examples of potential applications are molecular sieving and filter membranes [1,2], ion exchanger [3,4], sensor systems [5], laser media [6–8], catalysts [9] or novel drug-delivery-systems [10,11].

\* Corresponding author. Address: Department für Chemie und Biochemie, Ludwig-Maximilians-Universität, München, Butenandtstrasse 11, 81377 München, Germany. Tel.: +49 89 2180 77547; fax: +49 89 2180 77548.

E-mail address: [Christoph.Brauchle@cup.uni-muenchen.de](mailto:Christoph.Brauchle@cup.uni-muenchen.de) (C. Bräuchle).

For most applications the interactions between the mesoporous host and the guest molecules play a crucial role. Whereas Ensemble-measurements like NMR [12], electron microscopy [13], X-ray diffraction or neutron scattering [14] provide only information about the mean behaviour of the host–guest system, single molecule spectroscopy (SMS) offers insight into heterogeneities of the system and mechanistic details of dynamic processes such as spectral [15], orientational [16–18], and lateral diffusion [19–22]. In a recent contribution we showed how single terylene diimide (AS-TDI, structure shown in Fig. 1c) molecules can be used to investigate hexagonal and lamellar phases of Brij-56 templated mesoporous thin films [22] (a scheme of the two topologies and the structure of the template molecule are shown in Fig. 1a). The dye molecules can be incorporated as guests in the template-filled channels of such mesostructured materials during the synthesis procedure. In such a system the microscopic environment of the guest molecules is complex: the template micelles act as solvent for the hydrophobic AS-TDI molecules and interactions with the silica walls occur during their walk [23]. Furthermore, small molecules coming from the surrounding atmosphere like water are

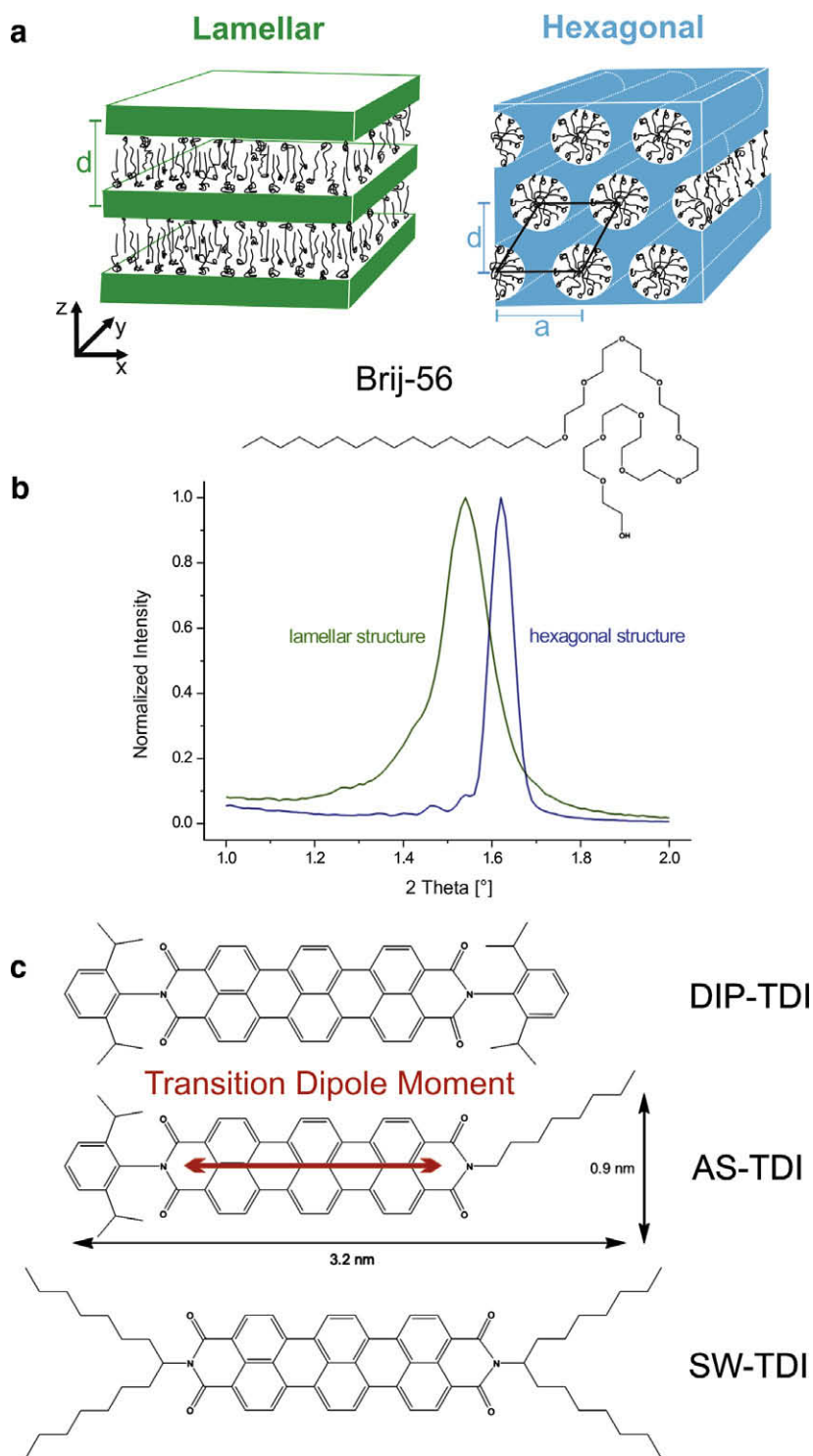


**Fig. 1.** Overview of the host-guest system. (a) Schematic diagrams of the lamellar (upper left panel) and the hexagonal (upper right panel) topologies and the respective arrangement of the template Brij-56 (structure shown in the lower panel). (b) Small-angle X-ray diffraction patterns of the two mesoporous structures exhibiting a sharp peak. The lamellar phase has a layer-to-layer distance  $d = 5.7 \pm 0.1$  nm, and for the hexagonal phase  $d = 5.5 \pm 0.1$  nm (pore-to-pore distance  $a = 6.3 \pm 0.1$  nm). (c) Structures of the three TDI derivatives: DIP-TDI, AS-TDI and SW-TDI.

always present in the channels, influencing the diffusion properties [24–26]. Hence, the single dye molecules act as ideal molecular probes providing structural as well as dynamical information about the host. For example, single AS-TDI molecules could be observed travelling in the different topologies of the host systems. It was even possible to distinguish AS-TDI molecules diffusing along the channels of the hexagonal phase from those that move very

slowly in the lamellar galleries. In addition, direct information about the dynamics inside of the host system could be obtained by analyzing the single molecule trajectories. In particular, the heterogeneities of the host systems are reflected by the complex modes of motions observed for the single guest molecules.

As the host-guest interactions are expected to strongly depend on the chemical nature of both host and guest, it is of great interest

to study the influence of the chemical structure of the guest molecules. This knowledge is crucial for most applications since these mesoporous systems are designed for incorporating various guest species. So far, we investigated the interplay between guest and host with the same guest molecule (AS-TDI) in different host systems [22]. AS-TDI is an asymmetric molecule based on a two-dimensional strongly fluorescent terylene diimide core with an octyl tail at one end of the molecule and an 2,6-diisopropyl-phenyl substituent at the other end. In this work we used SMS to investigate the orientational and translational dynamics of three different TDI derivatives diffusing in hexagonal and lamellar phases of Brij-56 templated mesoporous films. The structural differences between the different TDI derivatives are based on the nature of the substituents (structures shown in Fig. 1b). DIP-TDI and SW-TDI are two symmetric molecules with two 2,6-diisopropyl-phenyl and two 1-heptyl-octyl substituents, respectively. The third TDI derivative is the asymmetric AS-TDI molecules already used. In the following, it will be shown how the different substituents influence the interactions between the different guest molecules and the template-filled pores and lamellas, leading to dramatically different diffusional as well as orientational behaviours of the dye molecules.

## 2. Experimental section

### 2.1. Synthesis

The silica films were prepared by Evaporation-Induced Self-Assembly (EISA). The precursor solutions were synthesized by mixing 2.08 g (0.01 mmol) tetraethyl orthosilicate (TEOS, Aldrich) with 3.00 g 0.2 M HCl, 1.80 g H<sub>2</sub>O and 7.90 g EtOH and heating at 60 °C for 1 h to prehydrolyze the silica precursor under acid-catalysed condition. Then 0.57 g or 2.72 g of the structure building agent Brij-56 in 7.80 g or 37.5 g EtOH were added to obtain a hexagonal or lamellar mesoporous structure, respectively. Moreover, 4 µl of a highly diluted solution (about 10<sup>-8</sup> M) of a terylene diimide (TDI) dye (AS-TDI, DIP-TDI or SW-TDI) was added to 1 ml of the precursor solutions. Finally, 80 µl of the solutions were spin-coated on previously cleaned glass substrates (Marienfeld, size 20 × 20 mm, thickness 170 µm) at 3000 rpm.

### 2.2. Ellipsometry

The thickness of the mesoporous films was obtained using a Woollam ESM-300 Ellipsometer.

### 2.3. X-ray diffractometry (XRD)

The structure of the mesoporous films was determined with a Scintag XDS 2000 diffractometer in Bragg-Bretano scattering geometry.

### 2.4. Wide-field microscopy and single particle tracking (SPT)

Fluorescence images were acquired with a wide-field setup, using a Nikon Eclipse TE200 epifluorescence microscope using an oil-immersion objective with high numerical aperture (Nikon Plan Apo 100×/1.40 N.A. Oil). The TDI dye molecules were excited at 633 nm with a Coherent He-Ne gas laser (75 mW max. at 632.8 nm) with an intensity of 0.3 kW cm<sup>-2</sup>. The Fluorescence was detected with an Andor iXion DV897 back-illuminated EM-CCD camera in frame transfer mode (512 × 512 px). Incident laser light was blocked by a dichroic mirror (640 nm cutoff, AHF) and a band-pass filter (730/140, AHF). More details about the setup have been reported previously.

Confocal Microscopy: measurement of the orientation of the different TDI derivatives in the lamellar phase. For the orientation measurements the mesoporous films were investigated with a modified inverted confocal laser scan microscope (ZEISS LSM 410). An oil-immersion objective with a high numerical aperture (ZEISS 63× 1.4 oil) and a 633 nm He-Ne laser were used for the excitation of the TDI dye molecules. The fluorescence light was separated from the laser light using a combination of filters consisting of a dichroic mirror (Q640LP AHF Analysentechnik) and a combination of two fluorescence filters (633 nm Notch Kaiser; HQ720/150 AHF Analysentechnik). The fluorescence is detected outside the microscope with a single photon counting avalanche photodiode (EG&G SPCM-AQ 141). For the measurements of the pure lamellar phase, the bottom of the substrate was embedded in water to obtain a better matching of the refractive indices. To measure the orientation, a rotating, broad band λ/2 plate, which is placed just before the objective, is used to modulate the polarization plane of the excitation light. The fluorescence intensity of the dyes is recorded in dependence of the polarization angle of the excitation light. The orientation of the TDI molecules in the focal plane was determined by fitting a cosine-squared function to the data from a region of interest of 16 × 16 pixels centered on the molecule according to

$$I = A_0 \cos^2(\omega t - \Phi_{\text{ref}} + \Phi_{\text{mol}}) \quad (1)$$

$A_0$  is the amplitude of the cosine-squared curve,  $\omega$  the angular rotation velocity of the λ/2 plate,  $\Phi_{\text{ref}}$  the phase of the modulated transmission signal and  $\Phi_{\text{mol}}$  the in-plane angle of the molecule. The zero value for the angle is given by the direction of the main axis of the polarizer, which corresponds here to the horizontal line in the confocal fluorescence images.

The transmission signal was used as reference to obtain the absolute angle of the transition dipole moment. It passed through a polarizer and was recorded simultaneously to the fluorescence signal. The sum of the pixel intensity values of the horizontal lines of the region of interest was plotted versus time, and was fitted with

$$I = A_1 \cos^2(\omega t - \Phi_{\text{ref}}) \quad (2)$$

$A_1$  is the amplitude of cosine-squared function,  $\omega$  the angular speed of the λ/2 plate and  $\Phi_{\text{ref}}$  the phase of the signal.

Experiments have been carried out with a pure lamellar phase film aligned perpendicular to the focal plane containing TDI molecules at high concentration (10<sup>-5</sup> M in the synthesis solution).

## 3. Results and discussion

The investigated mesoporous silica materials were synthesized as thin films by spontaneous self-assembly of template and polymerisable silica precursor molecules [27]. Depending on the surfactant/silica molar ratio, we could produce either hexagonal or lamellar phases (for details see Section 2). The different TDI molecules were inserted at very low concentration (10<sup>-10</sup> M) in the synthesis solutions of the mesoporous films to ascertain single molecule observation.

X-ray diffractometry (XRD) was first used to determine the structure of the mesoporous films. Typical X-ray diffractograms are shown in Fig. 1b for a hexagonal and a lamellar topology (blue<sup>1</sup> and green plots, respectively). Both curves exhibit a sharp peak, indicating that the hexagonal and lamellar mesoporous phases are well structured. The 2θ values of the peaks can be used to cal-

<sup>1</sup> For interpretation of color in Figs. 1–3, the reader is referred to the web version of this article.



culate the average pore-to-pore distance  $a$  and the layer-to-layer distance  $d$  (see Fig 1a). In the case of the hexagonal phase we find  $2\theta = 1.62^\circ$ , which results in  $a = 6.3 \pm 0.1$  nm and  $d = 5.5 \pm 0.1$  nm. For the lamellar phase the  $2\theta$  value of the maximum is  $2\theta = 1.54^\circ$ , resulting in a layer-to-layer distance  $d = 5.7 \pm 0.1$  nm. As in these systems the wall thickness lies typically in the range of 1–2 nm, the pore diameter of the hexagonal structure would amount to about 4–5 nm, while the spacing of the lamellas is about 0.5 nm smaller. These values, however, can vary with time due to silica condensation leading to shrinkage of the mesoporous films [28]. Hence, all measurements presented here were carried out at the same time (2 days after synthesis) to assure comparability. X-ray diffractometry is a typical ensemble method which does not provide any information about the host–guest interactions and dynamics. Therefore, we used SMS to overcome this drawback.

Wide-field microscopy was performed to collect the fluorescence signal of the dye molecules and monitor their pathways inside the porous systems. Series of 1000 frames were recorded with a temporal resolution of down to 100 ms per frame. The inset in Fig. 2a shows a typical fluorescence image extracted from a movie of DIP-TDI molecules travelling in a hexagonal mesoporous phase. The single dye molecules appear as bright spots on a dark background. Single particle tracking (SPT) was employed to follow the molecules over all frames of the movies to obtain the single trajectories by fitting frame by frame theoretical diffraction patterns to the spots. With this method the positions of the fluorophores can be obtained with an accuracy of down to 10 nm [29]. Here we present first the results for the single molecule diffusion of the three TDI derivatives in the hexagonal phase, and then discuss the translational diffusion as well as the orientational behaviour of the guest molecules in the lamellar samples.

Fig. 2 shows the results for the hexagonal samples. Movies 1–3 (in Supplementary Material) show the diffusion in hexagonal samples of single DIP-TDI, AS-TDI and SW-TDI molecules, respectively. Similarly to what is observed in Fig. 2a for DIP-TDI, the single molecules of AS-TDI and SW-TDI appear solely as Gaussian-shaped diffraction patterns in the wide-field movies. Another immediate observation is that all the three TDI-dyes exhibit a very structured diffusional behaviour. A typical trajectory is displayed in Fig. 2a for DIP-TDI. The pathway of the molecule can be nicely followed as it explores the nanochannel system. This provides detailed information about the host structure such as sizes of domains of parallel pores and can reveal the presence of defects within the host structure like dead ends (green arrow) where the pores are closed. Also small openings have to be present in the silica walls (red arrow) through which the dye molecule can move to neighbouring channels as seen in high resolution experiments [30]. A statistical analysis based on the mean-square displacements (MSD) was performed for about 250 single molecule trajectories of each TDI derivative. For clarity, only the average MSD over all trajectories is plotted versus time in Fig. 2b for DIP-TDI (blue line), AS-TDI (red line) and DIP-TDI (green line). From this graph it becomes apparent that for short time lags the MSDs of each dye are linear and well separated, and for large time intervals they bend towards the similar horizontal asymptote at about  $200,000 \text{ nm}^2$ . This behaviour is characteristic for confined diffusion and does not just reflect the channel curvature since we found nearly perfectly linear trajectories exhibiting a similar bending of the MSD plot. It is known that the hexagonal mesoporous structures are organized in small domains of parallel channels [31–33]. Such domains correspond to the confinement regions, which is confirmed by the fact that the confinement areas of all the trajectories are in the same order of magnitude giving directly the typical domain size. The diffusion coefficients for each individual trajectory can be extracted from the linear part of the MSD plots according to the Einstein–Smoluchowski relation,

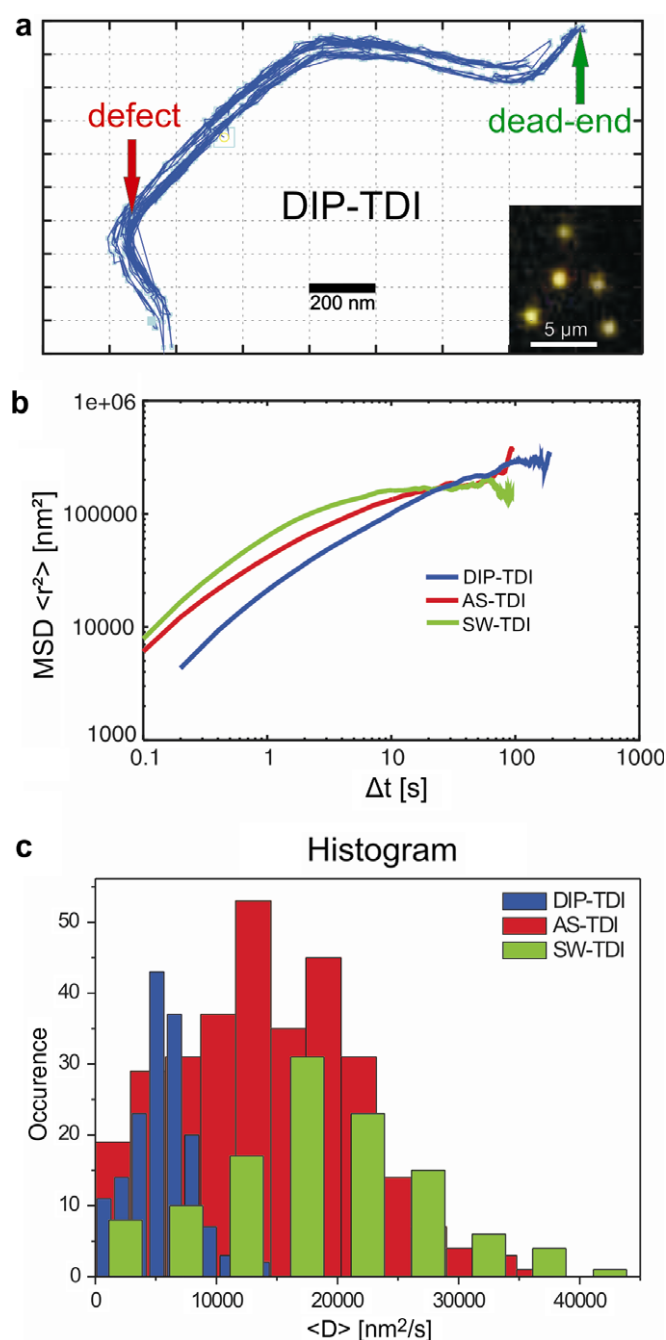


**Fig. 2.** Diffusional behaviour of the three TDI-dyes in the hexagonal pore system. (a) Highly structured trajectory of a single DIP-TDI molecule travelling inside the hexagonal channels. The insert displays a wide-field fluorescent image extracted from a movie (Movie 1 in Supplementary Materials) showing single DIP-TDI molecules diffusing in a hexagonal mesoporous film. (b) Mean square displacements (MSD) versus time averaged over about 250 single molecules trajectories for DIP-TDI (blue line), AS-TDI (red line) and SW-TDI (green line). (c) Histogram of the mean diffusion coefficients  $D$  extracted from the linear part of the individual MSD plots for the three TDI derivatives.

$$\text{MSD} = 4Dt \quad (3)$$

assuming a two-dimensional Brownian diffusion for the step sizes much smaller than the confinement area (in this case the ten first step sizes were taken into account). Fig. 2c displays the histograms of the diffusion coefficients for all the single trajectories of the three TDI conjugates. Clearly, the distributions are well separated with the trend for the diffusion coefficients:  $\langle D \rangle_{\text{SW-TDI}} > \langle D \rangle_{\text{AS-TDI}} > \langle D \rangle_{\text{DIP-TDI}}$ .

**Table 1**  
Diffusion coefficients and standard deviations of the three TDI derivatives in the hexagonal phase.

Dye	$\langle D \rangle$ [ $\text{nm}^2/\text{s}$ ]
DIP-TDI	$(0.6 \pm 0.2) \cdot 10^4$
AS-TDI	$(1.3 \pm 0.9) \cdot 10^4$
SW-TDI	$(1.9 \pm 0.7) \cdot 10^4$

The mean diffusion coefficients and their standard deviations are shown in Table 1.

The differences between the diffusion coefficients of the different TDI-dyes are induced by the different interactions of the substituents with the template molecules and the silica walls. It is known that the guest molecules can interact strongly with the silica walls of the mesoporous host structure at adsorption sites such

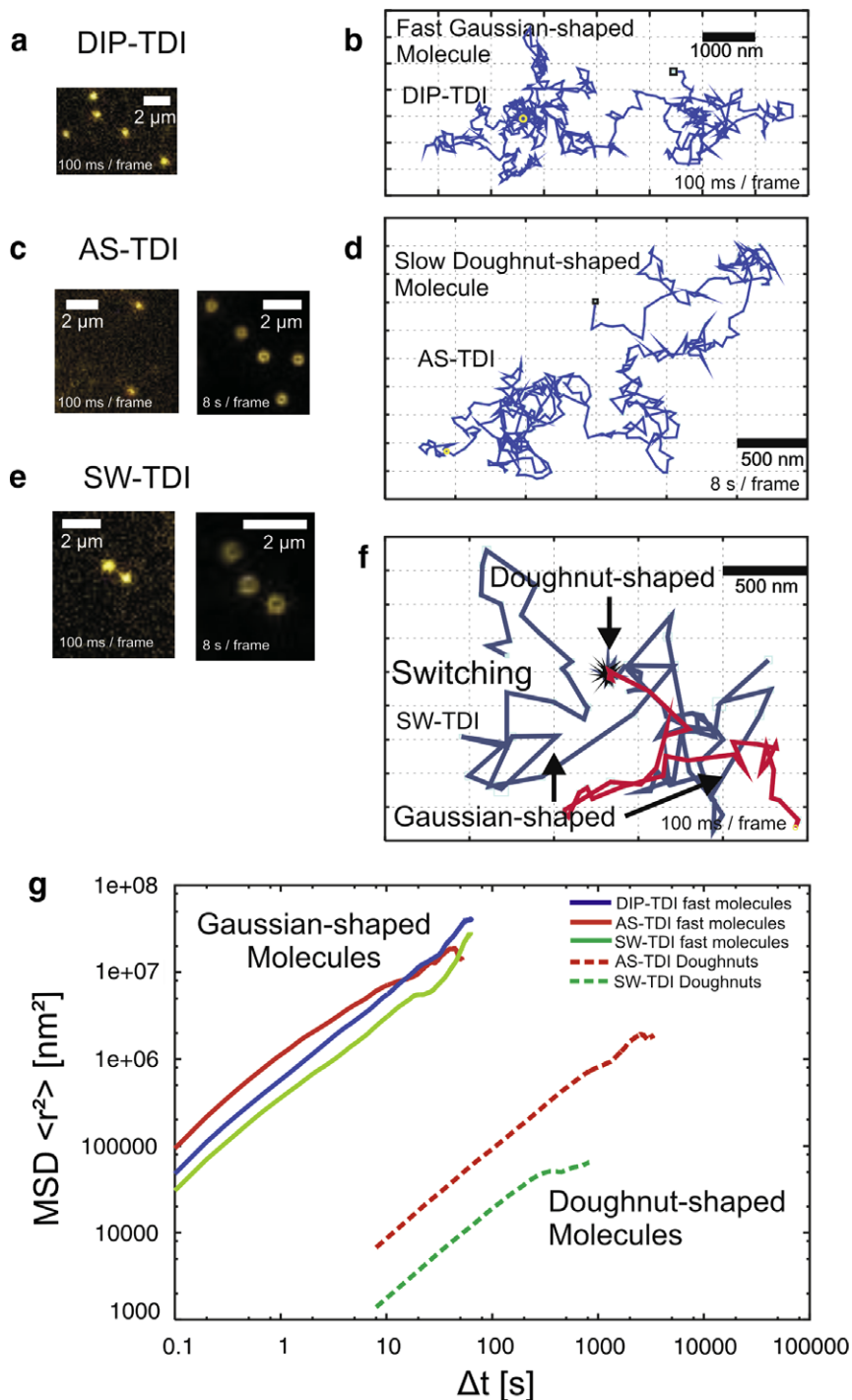


**Fig. 3.** Diffusional and orientational behaviour of the three TDI-dyes in the lamellar structure. (a) Wide-field fluorescence images of single DIP-TDI molecules acquired with 100 ms/frame. (b) Trajectory of a fast Gaussian-shaped DIP-TDI molecule travelling randomly inside the template-filled lamellas. (c) Wide-field images of single AS-TDI molecules diffusing in a lamellar phase acquired with 100 ms/frame (left panel) and 8 s/frame (right panel) showing Gaussian- and doughnut-shaped molecules, respectively. (d) Unstructured trajectory of a slow, z-oriented AS-TDI doughnut-shaped molecule. (e) Wide-field images of single SW-TDI molecules acquired with 100 ms/frame and 8 s/frame. (f) Individual SW-TDI molecule undergoing switches between Gaussian- (red and blue tracks) and Doughnut-shaped pattern (black track). (g) Mean square displacements (each curve averaged over about 30 single molecule trajectories) for the three TDI conjugates diffusing in the lamellas. Two populations can be distinguished: Fast molecules with Gaussian-shaped patterns (straight lines) and slow molecules with doughnut-shaped patterns (dotted lines).

as silanol groups [2,23–25,34]. This phenomenon hinders the diffusion, giving rise to lower diffusion coefficients. SW-TDI, with four alkyl chains, is expected to dissolve better than AS-TDI (with only one alkyl chain) in the cylindrical micelles of Brij-56. Hence, the tendency to adsorb occasionally to the silica walls is lowered, leading to a higher diffusion coefficient. DIP-TDI, with no alkyl chains, has consequently the lowest mean diffusion coefficient. The standard deviations given in Table 1 were obtained from the width of the Gaussian fit of the histograms in Fig. 2c. They reflect the presence of heterogeneities in the system, e.g. of the silica matrix, template arrangement or structure of the guest molecule.

Whereas different TDI structures result mainly in different diffusion coefficients in the hexagonal phase, the picture is much more complex with the lamellar samples. Fig. 3a shows a frame extracted from a sequence of wide-field fluorescence images (Movie 4 in Supplementary Material) acquired with a time resolution of 100 ms/frame, and showing single DIP-TDI molecules diffusing in a lamellar phase. The dye molecules appear with the typical Gaussian-shaped diffraction patterns, and exhibit a fast, totally unstructured diffusion. Fig. 3b displays an exemplary trajectory of such a DIP-TDI molecule diffusing in a random manner. This stands in contrast with the highly structured trajectories obtained in the hexagonal phase (illustrated in Fig. 2a), and is consistent with the random motion in the surfactant layers between the silica planes which allows two-dimensional diffusion. For AS-TDI and SW-TDI, the picture becomes more complicated. Indeed, the observation of the wide-field images of these two conjugates in the lamellar topologies reveals the presence of two populations of single molecule patterns as can be seen in Fig. 3c and e (frames extracted from Movies 5 and 7 for AS-TDI, and Movies 6 and 8 for SW-TDI in Supplementary Materials). One population exhibits fast and the other one slow diffusion. Therefore, these fluorescence images recorded from the same sample of a given TDI derivative were measured with two different integration times (100 ms/frame for the left panels; 8s/frame for the right panels) which allows resolving the dynamics occurring at different timescales. The two movies acquired with short integration time (100 ms/frame) show for both dyes fast, randomly diffusing molecules appearing with Gaussian-shaped diffraction patterns, similarly to what was observed with DIP-TDI. In contrast, in the movies acquired with longer integration time (8 s/frame) the single molecules appear as doughnuts. Such doughnut-shaped diffraction patterns have been previously reported in the lamellar phase for AS-TDI [22] and have been assigned to single molecules whose transition dipole moment (for TDI conjugates the long molecular axis) is constantly aligned along the optical axis of the microscope. This means that these molecules are oriented perpendicular to the glass substrate and thus normal to the silica planes of the lamellar phase. An additional observation is that the doughnuts move in a random way similarly to the Gaussian-shaped molecules as can be seen in the trajectory displayed in Fig. 3d. However, the diffusion of the doughnuts is much slower according to the 80-times longer integration time. In our previous work we explained the preferential z-orientation of the doughnuts by strong interactions between the AS-TDI molecules and the template molecules. This results in the alignment of the AS-TDI molecules along the template chains, i.e. perpendicular to the silica layers. Obviously, in the case of DIP-TDI these interactions are not strong enough to be able to orient the molecules, which is probably due to the absence of an alkyl tail in the guest structure. Hence, the DIP-TDI molecules are able to take different orientations within the surfactant-filled layers. In the case of SW-TDI which have four alkyl chains we observe behaviour similar to the one of AS-TDI. Indeed, two populations of diffusing molecules are observed: fast Gaussian-shaped molecules and slow doughnut-shaped molecules oriented perpendicular to the mesoporous film.

In summary, DIP-TDI molecules diffusing in a lamellar phase exhibit Gaussian-shaped patterns, whereas for AS-TDI and SW-TDI one can distinguish two sub-populations of diffusing single molecules: fast Gaussian-shaped and slow doughnut-shaped molecules oriented perpendicular to the silica planes. We estimated roughly the ratio of the two populations by counting the number of Gaussian- and doughnut-shaped molecules (see Table 2).

Hence, while no doughnut at all could be observed with DIP-TDI, the AS-TDI molecules exhibit about 90% doughnuts, and in the case of SW-TDI we found a ratio of about 1:1 for the two populations.

Interestingly, transitions between the sub-populations could even be observed for AS-TDI as well as for SW-TDI. This is illustrated in Fig. 3f which shows the trajectory of a single SW-TDI molecule travelling at first rapidly with a Gaussian-shaped pattern (red track), and after 8.6 s switches its shape into a doughnut (black) being nearly immobile at this integration time (100 ms/frame). Then, 12.7 s later, the molecule's shape changes again into a Gaussian-shaped pattern diffusing fast again (blue track). Such switches transforming fast Gaussian-shaped molecules into slow doughnuts and the other way round are encountered occasionally (roughly one switching event is observed after 2 min of observation time for about 20% of the molecules, the other molecules showing no switching event). They indicate a sudden change in the orientation of the molecules accompanied with a dramatic change of the diffusion coefficient.

The average MSDs for the Gaussian- and the doughnuts-shaped molecules are plotted in Fig. 3g for DIP-TDI (blue line), AS-TDI (full and dotted red lines, respectively), and SW-TDI (full and dotted green lines, respectively). All the MSD plots are linear, confirming that the diffusion behaviour of both populations for the three TDI derivatives can be described by two-dimensional random walks. The mean diffusion coefficients were obtained with linear fits of the MSD plots according to Eq. (3) and are shown in Table 3.

Overall, the diffusion coefficients of the fast TDI molecules with Gaussian-shaped patterns in the lamellar structure are about one order of magnitude higher than in the hexagonal pores. This may be explained by the more dense packing of the surfactant molecules in the hexagonal phase leading to a more viscous medium. Indeed, a perfect coverage of the silica walls with template molecules would result in a much higher density of the alkyl chains of Brij-56 in the middle of the pore due to the cylindrical geometry in the hexagonal phase. However, the trend in the lamellar phase ( $\langle D \rangle_{AS-TDI} > \langle D \rangle_{DIP-TDI} > \langle D \rangle_{SW-TDI}$ ) is also different than in the hexag-

**Table 2**

Ratio of fast Gaussian-shaped molecules to slow Doughnut-shaped molecules for the three TDI-dyes in the lamellar phase.

Dye	Ratio (Gaussian-shaped molecules (fast)/Doughnut-shaped molecules (slow)) [%]
DIP-TDI	100:0
AS-TDI	10:90 [35]
SW-TDI	45:55

**Table 3**

Diffusion coefficients and standard deviations of the three TDI derivatives in the lamellar phase.

Dye	Gaussian-shaped molecules		Doughnut-shaped molecules
	$\langle D \rangle$ (nm <sup>2</sup> /s)	$\langle D \rangle$ (lam)/ $\langle D \rangle$ (hex)	$\langle D \rangle$ (nm <sup>2</sup> /s)
DIP-TDI	$(1.6 \pm 0.5) \cdot 10^5$	26.7	–
AS-TDI	$(2.8 \pm 0.7) \cdot 10^5$	17.5	230 ± 120
SW-TDI	$(0.8 \pm 0.4) \cdot 10^5$	4.2	65 ± 82



onal phase ( $\langle D \rangle_{\text{SW-TDI}} > \langle D \rangle_{\text{AS-TDI}} > \langle D \rangle_{\text{DIP-TDI}}$ ). Indeed, the ratio between the diffusion coefficients in the lamellar and the hexagonal phase ( $\langle D \rangle_{\text{lam}} / \langle D \rangle_{\text{hex}}$ ) is very different for the three TDI derivatives as shown in Table 3. Whereas DIP-TDI diffuses 26.7 times faster in the lamellar than in the hexagonal structure, AS-TDI diffuses 17.5 times faster and SW-TDI only 4.2 times.

In particular, SW-TDI, which was the fastest dye inside the hexagonal pores, becomes the slowest one between the lamellas. These strong differences in the diffusional behaviour are unexpected, and are likely caused by the different geometry of the silica structure as well as the template's arrangement in the lamellar phase, which may induce different host-guest interactions. For example, the alkyl chain of AS-TDI might interact stronger with the parallel alkyl chains of the template in the lamellar phase than with the radial oriented template in the hexagonal phase. Hence, the movement of the dye is hindered in the lamellar phase compared to DIP-TDI, which has no alkyl chain. This effect seems even stronger for SW-TDI, whose all four alkyl chains might even align parallel to the template molecules in the lamellar structure.

Furthermore, another striking observation is that the diffusion coefficients of the doughnuts are about three orders of magnitude lower than those of the Gaussian-shaped molecules. The AS-TDI and SW-TDI doughnuts are most probably hindered in their movement by strong interactions with the surfactant molecules aligned parallel. This assumption is supported by the 3.5 times lower diffusion coefficient of the doughnuts of SW-TDI compared to those of AS-TDI (230 nm<sup>2</sup>/s and 65 nm<sup>2</sup>/s, respectively). Indeed, it is expected that the four chains of SW-TDI induce more interactions with the template molecules than the single octyl chain of AS-TDI, hence hindering the movement. Finally, for the Gaussian-shaped molecules in the lamellar phase the same trend for the diffusion coefficients was observed:  $D_{\text{AS-TDI}} > D_{\text{SW-TDI}}$ . This is a hint, that for the two populations the relative interactions of AS-TDI and SW-TDI molecules with the template are similar and depend only on the structures of the dye molecules, i.e. in this case on the alkyl chains. Therefore SW-TDI molecules holding four alkyl chains present stronger interactions with the alkyl chains of the template than AS-TDI with only one alkyl chain and consequently being slowed down in a stronger way.

The presence of two populations of diffusing molecules in the lamellar phase as well as of switching events between those is quite surprising. The wide-field measurements indicate already that the two populations exhibit a different orientational behaviour. It has also been shown that for one population the TDI molecules are oriented perpendicular to the substrate, showing up as doughnut diffraction limited patterns. However, the orientation of the fast molecules forming the second population is not known exactly. To gain a deeper insight, polarization modulation dependent confocal microscopy was used to measure the orientational behaviour of the TDI conjugates in the lamellar phase. Hence, a sample was observed from the side in order to obtain a better excitation of the fluorophores, especially of the doughnuts (see Fig. 4a). The dye molecules were embedded in the mesoporous film at ensemble concentration to provide a sufficient fluorescence signal in this geometry, and the excitation polarization of the laser was rotated continuously (for details see Section 2).

Fig. 4b (left panel) shows an excerpt extracted from the fluorescence image of a lamellar phase loaded with DIP-TDI. The mesoporous film appears here as a bright, homogeneous fluorescence signal. As the excitation polarization of the laser was rotated continuously during the confocal scan this means that the transition dipole moments of the DIP-TDI molecules point in every direction, and consequently has no preferential orientation. This is consistent with the wide-field measurement in which the single DIP-TDI molecules appear only as Gaussian-shaped patterns. These observations suggest that the DIP-TDI is able to rotate freely within the

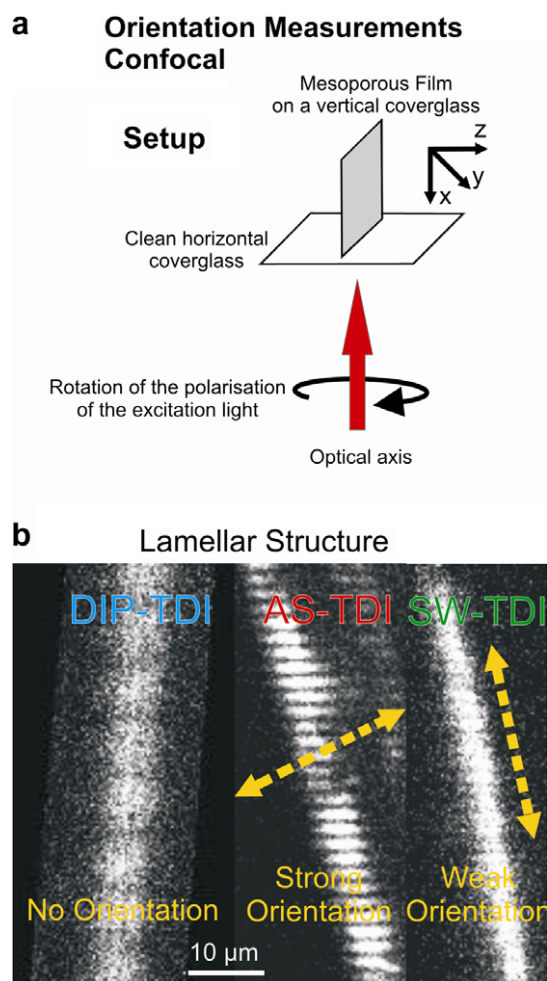


**Fig. 4.** Measurements of the orientation of the TDI conjugates in the lamellar phase. (a) Sketch of the alignment of the lamellar film perpendicular to the focal plane. (b) Polarization modulated confocal images for DIP-TDI (left panel), AS-TDI (middle panel), and SW-TDI (right panel) inside the lamellar phase. Whereas DIP-TDI exhibits a homogeneous fluorescence signal indicating that its molecules can rotate freely inside the lamellas, the AS-TDI shows a striped fluorescence pattern which reveals an overall strong orientation perpendicular to the silica lamellas. In the case of SW-TDI, the fluorescence signal is only weakly polarized, indicating a more complex orientational behaviour (see text for details).

lamellas. Indeed, the inter-plane distance, estimated to be 3.7–4.7 nm, provides enough space for the DIP-TDI molecules (about 3 nm in length) to reorient their dipole moments. This also indicates that the interactions with the template are most probably much weaker than for AS-TDI and SW-TDI, probably because of the absence of alkyl chains in the structure of DIP-TDI.

In contrast, the fluorescence of the mesoporous film loaded with AS-TDI appears as a thin, striped vertical line, as shown in Fig. 4b (middle panel). This reveals that the AS-TDI dye molecules are not oriented randomly within the lamellar phase, but are mostly aligned in the same direction. This was indeed expected as most of the molecules appear as doughnuts in the wide-field images. To determine the average direction of the alignment the modulation of the transmission light was detected behind a fixed polarizer and acts as a reference for the determination of the angles (the angle of a horizontal line in Fig. 4b is set to 0°). Both fluorescence and reference images were used to determine the orientation at several chosen positions (for details, see Section 2). The average extracted angle is  $15^\circ \pm 3^\circ$ , which is the mean angle of the distribution of the orientations of the transition dipole mo-



ments of the AS-TDI molecules. This angle corresponds exactly to the direction perpendicular to the mesoporous film and thus perpendicular to the silica planes of the lamellar phase, which is consistent with the z-oriented doughnuts observed in the wide-field movies. However, the orientation of the other population of Gaussian-shaped pattern molecules could not be determined by the confocal measurements. As AS-TDI was used at an ensemble concentration, this population constituted by only 10% of the molecules shows much weaker fluorescence intensity than the other population which is overlaid in the fluorescence image, and hence can not be easily detected. However there are two possibilities for the configuration for the transition dipole moment of these molecules leading to Gaussian-shaped patterns in the wide-field movies:

- The AS-TDI molecules constantly reorient their transition dipole moment, similarly to the DIP-TDI molecules.
- Their transition dipole moment remains in the *xy* plane of the wide-field setup, i.e. in the silica planes.

For SW-TDI, the fluorescence image (Fig. 4b, right panel) shows a slightly striped line, indicating only a partial orientation of the dye molecules. Surprisingly, in this case the extracted angle corresponds to the direction of the mesoporous film plane ( $99^\circ \pm 3^\circ$ ). From the wide-field measurements it was expected that the doughnuts would cause an overall orientation perpendicular to the lamellas of the mesoporous film, similarly to what was observed for AS-TDI. We suggest that the different orientation observed with the confocal setup arise from the other population which is constituted by the Gaussian-shaped molecules. The only possible configuration for these SW-TDI molecules which can explain the overall orientation along the film is an alignment of their transition dipole moment parallel to the lamellas. However, a condition for such an orientation is that these molecules are brighter than those of the other population. This condition could be fulfilled if the molecules of the two populations couple differently to their direct surrounding. For example, different interactions with the template or the silica walls might provide two distinct environments for the two configurations of TDI molecules. Furthermore, at ensemble concentration inter-molecular interactions might occur between the guest molecules and influence the ratio of the two populations of diffusing molecules compared to the single molecule concentration. Hence, it is possible that much more fast diffusing Gaussian-shaped SW-TDI molecules are present at ensemble concentration resulting in a brighter fluorescence signal for this population.

Altogether, these results enable us to suggest a picture of the behaviour of the three TDI-dyes in the lamellar structure, as depicted schematically in Fig. 5. The DIP-TDI molecules do not keep a preferential orientation, but constantly reorient during their walk within the template-filled lamellas (see Fig. 5a). In this system the host–guest interactions are probably relatively weak and do not influence the orientation of the DIP-TDI molecules significantly.

In contrast, 90 % of the AS-TDI molecules align along the template molecules due to strong interactions, and diffuse slowly in this configuration appearing as doughnuts in the wide-field movies. The other 10 %, the fast Gaussian-shaped molecules, may rotate freely, similarly to DIP-TDI. Another possibility for their transition dipole moment is to lie between the silica planes, as can be seen in Fig. 5b.

Finally, the SW-TDI molecules exhibit two distinct preferential orientations with about equal ratio. The first population (the doughnuts in the wide-field movies) corresponds to molecules oriented perpendicular to the lamellas, whereas the transition dipole moment of the molecules of the second population (Gaussian-shaped patterns) remains in the lamellar planes during their walk.

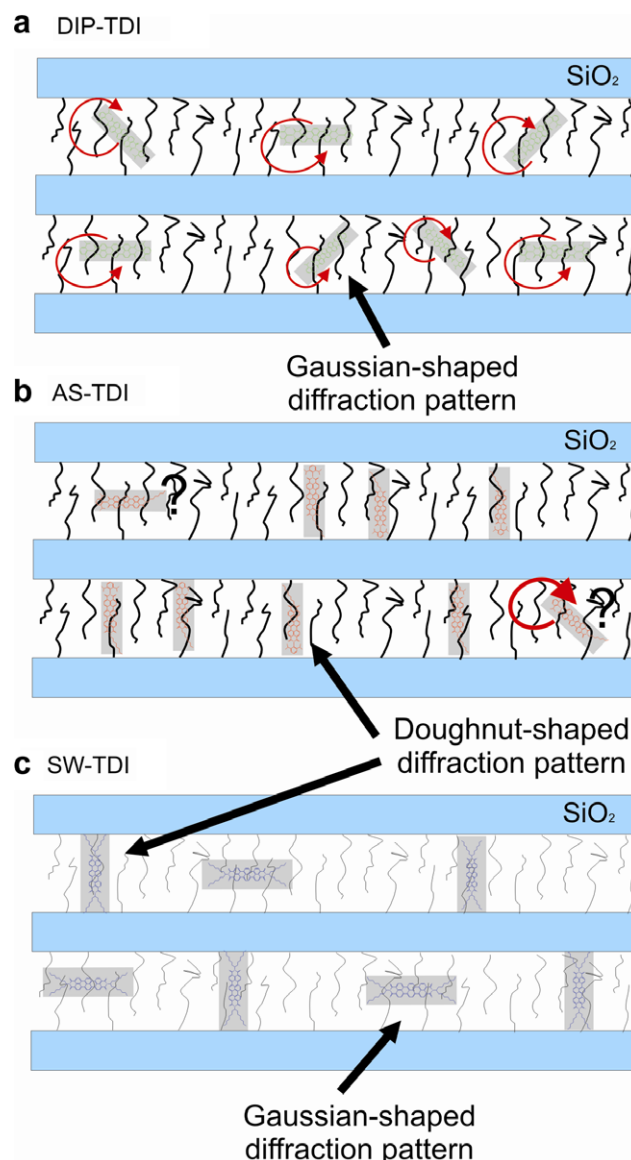


**Fig. 5.** Schematic of the proposed orientational behaviour in the lamellar structure for the three TDI derivatives. (a) The DIP-TDI molecules undergo constant reorientation of their transition dipole moment during their walk. (b) For AS-TDI two populations of diffusing molecules are observed: the slow doughnuts oriented perpendicular to the silica walls, and the Gaussian-shaped pattern molecules which are either freely rotating or whose orientation lies parallel to the silica planes. (c) In the case of SW-TDI two populations are also observed: the z-oriented doughnuts similarly to AS-TDI, and the Gaussian-shaped pattern molecules lying in the plane of the silica layers.

Strong interactions between the four alkyl tails of SW-TDI and the template molecules are assumed to dictate these two preferential configurations. Moreover, switches between these two populations can occur, as already mentioned. This shows that although the two populations refer to two energetically favoured orientations, the molecules are able to overcome the energetic barriers occasionally, maybe at defect sites in the silica walls or in the template of the host structure. It is also interesting to note that although SW-TDI has more alkyl chains and should align better with the template molecules than AS-TDI, the ratio of doughnuts to fast molecules is surprisingly smaller than for AS-TDI. An explanation might be that a configuration parallel to the lamellas is energetically more favourable for SW-TDI than for AS-TDI due to stronger interactions between the four alkyl chains and the template molecules. Nevertheless, other effects may also have to be considered. In the case of

SW-TDI for instance, sterical hindrance due to interactions between the four long alkyl chains and the silica walls in the doughnut configuration may explain the smaller ratio of doughnuts. In summary, the presence of one or more alkyl chains in the structure of TDI has a tremendous influence on the orientational behaviour of the guest molecules.

#### 4. Conclusion

Wide-field microscopy was used to investigate the dynamics of single molecules of three different TDI derivatives incorporated as guests in mesoporous silica host systems. The dye molecules are dissolved in the micelles of the template with occasional interactions with the silica walls of the pores during their walk. The diffusional behaviour in the hexagonal phase differs dramatically from unrestricted diffusion, e.g. in a liquid medium, as the motion of the single molecules is confined in the host channels. For the three TDI derivatives the highly structured trajectories reveal details about the underlying host structure like domain sizes, connectivity between the different channels, the presence of defects sites like holes in the silica wall or dead ends where the pores are closed. Moreover, dynamical information could be obtained. The three TDI conjugates show clearly distinct mean diffusion coefficients (with  $\langle D \rangle_{\text{SW-TDI}} > \langle D \rangle_{\text{AS-TDI}} > \langle D \rangle_{\text{DIP-TDI}}$ ) caused by the presence of different substituents in the guest molecules.

The behaviour of the TDI molecules differs dramatically in the lamellar host structure compared to the hexagonal phase. Whereas DIP-TDI exhibits only one population of diffusing molecules with Gaussian-shaped diffraction pattern, two sub-populations have been observed for AS-TDI and SW-TDI: fast diffusing molecules with Gaussian-shaped patterns and slowly diffusing molecules with doughnut-shaped patterns. For both populations, the single dye molecules diffuse in a random walk, contrasting with the highly structured trajectories in the hexagonal phase. Furthermore, information about the orientational behaviour of the different TDI molecules could be gathered. Whereas the Gaussian-shaped molecules of DIP-TDI reorient constantly during their walk in the lamellar galleries, AS-TDI and SW-TDI exhibit two different orientational behaviours. The molecules with doughnut-shaped patterns were attributed to molecules whose transition dipole moment is oriented perpendicular to the lamellas due to interactions between the alkyl chains of AS-TDI and SW-TDI with the template molecules. The faster Gaussian-shaped molecules of SW-TDI are probably oriented parallel to the lamellas, whereas in the case of AS-TDI either free rotation or an orientation of the transition dipole moment lying parallel to the silica planes are possible. Finally, transitions between the two orientational states were observed occasionally at the single molecule level. To conclude, this contribution is the first step in designing guests with adapted diffusion properties in order to gain better control over the host–guest interactions.

#### Acknowledgments

We thank the group of T. Bein (LMU, Munich, Germany) for providing the recipes for the synthesis of the mesoporous films and for supplying the facility for the XRD-measurements. This work was funded by the SFB 486, the SFB 749 and the Nanosystems Initiative Munich (NIM).

#### Appendix A. Supplementary data

Supplementary data associated with this article can be found, in the online version, at doi:10.1016/j.micromeso.2009.01.024.

#### References

- [1] M.J. Wirth, R.W.P. Fairbank, H.O. Fatunmbi, *Science* 275 (1997) 44.
- [2] M.J. Wirth, D.J. Swinton, M.D. Ludes, *J. Phys. Chem. B* 107 (2003) 6258.
- [3] M. Jaroniec, *J. Am. Chem. Soc.* 124 (2002) 14506.
- [4] H.G. Karge, H.K. Beyer, *Solid-State Ion Exchange in Microporous and Mesoporous Materials, Molecular Sieves – Science and Technology*, Springer, Berlin/Heidelberg, 2002.
- [5] P.C. Pandey, S. Upadhyay, H.C. Pathak, *Sensors Actuat. B: Chem.* 60 (1999) 83.
- [6] R. Reisfeld, *J. Lumin.* 72–74 (1997) 7.
- [7] P. Yang et al., *Science* 287 (2000) 465.
- [8] Ö. Weiss, J. Loerke, U. Wüstefeld, F. Marlow, F. Schüth, *J. Solid State Chem.* 167 (2002) 302.
- [9] A. Corma, *Chem. Rev.* 97 (1997) 2373.
- [10] C.-Y. Lai et al., *J. Am. Chem. Soc.* 125 (2003) 4451.
- [11] I. Roy et al., *PNAS* 102 (2005) 279.
- [12] V. Kukla et al., *Science* 272 (1996) 702.
- [13] O. Terasakis, Z. Liu, T. Ohsuna, H.J. Shin, R. Ryoo, *Microsc. Microanal.* 8 (2002) 35.
- [14] N.E. Benes, H. Jobic, H. Verweij, *Micropor. Mesopor. Mater.* 43 (2001) 147.
- [15] T. Basché, S. Kummer, C. Bräuchle, *Nature* 373 (1995) 132.
- [16] S. Megelski et al., *J. Phys. Chem. B* 105 (2001) 25.
- [17] A.P. Bartko, R.M. Dickson, *J. Phys. Chem. B* 103 (1999) 11237.
- [18] C. Jung, C. Hellriegel, J. Michaelis, C. Bräuchle, *Adv. Mater.* 19 (2007) 956.
- [19] C. Seebacher et al., *J. Phys. Chem. B* 106 (2002) 5591.
- [20] M.J. Saxton, K. Jacobsen, *Annu. Rev. Biophys. Biomol. Struct.* 26 (1997) 373.
- [21] J. Schuster, F. Cichos, C.v. Borczykowski, *J. Phys. Chem. A* 106 (2002) 5403.
- [22] J. Kirstein et al., *Nat. Mater.* 6 (2007) 303.
- [23] C. Jung et al., *JACS* 129 (2007) 5570.
- [24] Y. Fu, M.M. Collinson, D.A. Higgins, *J. Am. Chem. Soc.* 126 (2004) 13838.
- [25] Y. Fu, F.M. Ye, W.G. Sanders, M.M. Collinson, D.A. Higgins, *J. Phys. Chem. B* 110 (2006) 9164.
- [26] T. Lebold et al., *Chem. Eur. J.* 15 (2009) 1661.
- [27] C.J. Brinker, Y. Lu, A. Sellinger, H. Fan, *Adv. Mater.* 11 (1999) 579.
- [28] D. Grosso, F. Babonneau, G.J.d.A.A. Soler-Illia, P.-A. Albouy, H. Amenitsch, *Chem. Commun.* 748 (2002).
- [29] C. Hellriegel, J. Kirstein, C. Bräuchle, *New J. Phys.* 7 (2005) 23.
- [30] C. Jung et al., *J. Am. Chem. Soc.* 130 (2008) 1638.
- [31] A. Zurner, J. Kirstein, M. Doblinger, C. Bräuchle, T. Bein, *Nature* 450 (2007) 705.
- [32] R. Bandyopadhyaya, E. Nativ-Roth, R. Yerushalmi-Rozen, O. Regev, *Chem. Mater.* 15 (2003) 3619.
- [33] M. Matheron et al., *J. Mater. Chem.* 15 (2005) 4741.
- [34] M.J. Wirth, M.D. Ludes, D.J. Swinton, *Anal. Chem.* 71 (1999) 3911.
- [35] The presence of the Gaussian-shaped AS-TDI molecules in the pure lamellar phase was overlooked in our previous publication [22] because of their small ratio compared to the doughnuts and the difficulty to distinguish them from molecules at the surface of the mesoporous films. Here, an additional experiment based on polymer coating clearly allowed a distinct differentiation (data not shown)